engineering proceedings

MDPI

Proceeding Paper

Neural Network Performance Analysis of Wave Energy Converters Operating in the European Coastal Waters †

Onea Florin, Eugen Rusu and Roberto-Adrian Dobri *

Department of Mechanical Engineering, Faculty of Engineering, "Dunarea de Jos" University of Galati, 800008 Galati, Romania; florin.onea@ugal.ro (O.F.); eugen.rusu@ugal.ro (E.R.)

* Correspondence: roberto.dobri@ugal.ro

† Presented at the 1st International Online Conference on Inventions—Energy Security and Sustainable Development, 25–26 June 2026; Available online: https://sciforum.net/event/IOCIV2026.

Abstract

The current work seeks to identify the most critical wave properties that may influence the performance of Wave Energy Converters (WECs) operating near several European marine sites. As an initial step, local wave resources were identified using three years of hourly ERA5 data (2023–2025), also known as ECMWF Re-analysis version 5. According to these findings, wave energy resources gradually decrease from north (Ireland) to south (Portugal), with substantially lower values projected near the GEROA site (France) in the Bay of Biscay. Five WECs were considered for each area, with monthly performance indicators. A neural network approach (11 predictors and three responses) was used to uncover a potential association between WEC performance and local wave conditions. In most circumstances, the average wave height and wave strength are the most essential factors. Although each WEC is defined by a different operating principle (e.g., point absorber, attenuator, terminator), the wave direction is not highlighted as a representative aspect. Finally, we may note that the current work is ongoing and is likely to make a substantial contribution to the field of WEC selection/optimisation.

Keywords: European nearshore; marine energy site; wave power; WEC; ERA5; neural network

1. Introduction

The transition towards low-carbon energy systems has intensified interest in marine renewable resources, among which ocean wave energy is distinguished by its high energy density and comparatively predictable temporal behaviour. Waves are generated primarily through the transfer of wind energy to the ocean surface and can transport substantial energy over long distances with limited dissipation. Global assessments indicate that the theoretical resource is sufficiently large to contribute meaningfully to electricity generation, particularly in coastal regions exposed to persistent wave climates. Nevertheless, wave energy remains less technologically mature than wind and solar power, while commercial deployment is constrained by technical complexity, high investment costs, difficult offshore maintenance, and the absence of convergence towards an optimal conversion technology [1–4].

Wave energy converters comprise a diverse group of devices designed to absorb the kinetic and potential energy of waves and transform it into electrical power. They may be classified according to location, orientation, or operating principle. Common concepts include oscillating water columns, overtopping devices, attenuators, terminators, and point

Check for updates

Academic Editor: Trilochan Bhatta

Published: 8 October 2026

Copyright: © 2026 by the authors. Licensee MDPI, Basel, Switzerland. This article is an open access article distributed under the terms and conditions of the Creative Commons Attribution (CC BY) license.

absorbers. Point absorbers have attracted particular attention because of their compact geometry, adaptability, and capacity to capture energy from different directions. Irrespective of the conversion principle, WEC performance results from the interaction among the hydrodynamic structure, power take-off system, electrical generator, control strategy, and power electronic interface. These components cannot be optimised independently because changes in one subsystem may alter the response and efficiency of the entire device [5]. The generator and power take-off stages are especially important because ocean waves produce slow, irregular, bidirectional motion accompanied by substantial force variations. This input must be converted into usable electrical energy while losses are minimised and reliable operation is maintained under variable sea states. WEC systems may employ rotary generators coupled to hydraulic or pneumatic turbines, or direct-drive linear generators that convert translational motion without an intermediate transmission. Permanent magnet synchronous machines, induction generators, switched reluctance machines, and linear permanent magnet generators have been examined for wave energy applications. Each solution differs in efficiency, controllability, structural complexity, maintenance requirements, and compatibility with variable-speed operation. Generator performance is therefore sensitive to wave characteristics, device geometry, power take-off parameters, control settings, and electrical loading conditions [2,5].

The nonlinear and strongly coupled behaviour of WEC systems makes comprehensive performance assessment difficult when conventional analytical or numerical models are used alone. High-fidelity hydrodynamic and electromagnetic simulations provide detailed information, but their computational cost may become prohibitive when many operating conditions and design variables are examined. Artificial neural networks offer an alternative framework capable of learning complex input-output relationships from numerical, experimental, or operational data. Recent research has demonstrated their potential for predicting WEC responses, supporting wave forecasting, optimising buoy geometry, and identifying configurations associated with improved energy capture. Neural-network-assisted buoy optimisation has also achieved high predictive accuracy for key hydrodynamic responses, indicating that data-driven models can serve as efficient surrogate tools during repeated design evaluations [3,4].

Within this context, sensitivity analysis provides a systematic means of determining how variations in environmental, mechanical, and electrical parameters influence generator response and predicted power production. Identifying the dominant variables can support model simplification, experimental planning, control development, and uncertainty reduction during WEC optimisation.

The overall effectiveness of a WEC system is typically used to demonstrate its performance, but the significance of particular wave properties is not always evident. The goal of the current work is to cover this gap by considering several coastal locales in Europe and WEC systems, which will be assessed using a neural network approach.

2. Materials and Methods

Figure 1 highlights the reference sites taken into account. The first one is associated with the Atlantic Marine Energy Test Site (IE24), which is located in western Ireland [6]. The second is located in the Bay of Biscay, namely near the Green Energy Research for Offshore Atlantic site (GEROA, Spain) [7]. Another notable location is Botafogo, Portugal, where a 990 MW offshore wind project is proposed [8]. Although these sites are located in the North Atlantic Ocean, each one is predicted to be defined by specific wave resources.

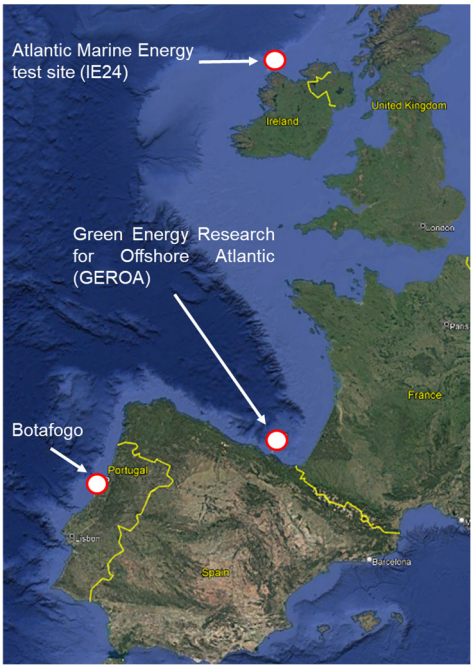

Figure 1. Reference sites considered for the assessment of WEC performances. Figure processed from Google Earth Pro, 2026 (version 156.0.8067.0).

The current work is based on the ERA5 hourly dataset [9], which spans the three-year period 2023–2025. The following criteria will be considered when assessing wave resources: (a) significant wave height (or *Hs*), (b) energy mean wave period (or *Te*), and (c) wave direction. The ERA5 reanalysis wave data are commonly used to evaluate the performance of WECs, as they are available on a worldwide scale and do not contain missing values.

Aside from the wave parameters, another essential element considered is the wave power, which for deep water locations can be defined as [10]:

$$P_w = \frac{\rho g^2}{64\pi} T_e H_s^2 \quad (1)$$

where P_w represents the energy flux (kW/m); ρ = 1025 kg/m^3 is the density of sea water; and g = 9.81 m/s^2, is the gravity acceleration.

Another goal of the current study is to estimate the performance of several WEC generators using various operating principles, such as point absorber, attenuator, or terminator [11]. Figure 2 highlights the WEC systems investigated for the present investigation, which include: Seabased (rated capacity: 15 kW, point absorber); Oceantec (500 kW, point absorber); Pelamis (750 kW, attenuator); and Wave Bob (1000 kW, point absorber); Wave Dragon (5900 kW, terminator). The literature review [12] provides additional information on these WECs.

The power output of a given WEC can be calculated by combining each generator's power matrices with a specific sea state bivariate distribution described by the *Hs* and *Te* parameters. This can be defined as [13]:

$$P_E = \frac{1}{100} \cdot \sum_{i=1}^{nT} \sum_{j=1}^{nH} PW_{ij} \cdot PM_{ij} \quad (2)$$

where PW_{ij} bivariate distribution is defined by line i and column j; and PM_{ij} is defined by the expected WEC power output related to the bivariate distribution. This parameter can be used to further estimate the capture width and capacity factor [14].

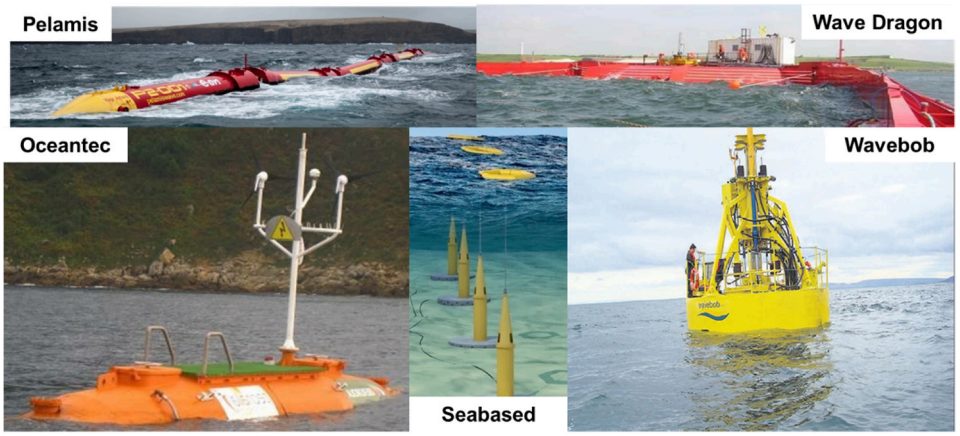

Figure 2. Overview of wave energy converters considered for evaluation.

Figure 3 highlights the method for Pelamis at the IE24 location in Ireland. Figure 3a depicts the Pelamis power matrix, whereas Figure 3b present the bivariate sea-state distribution organised using the same wave-height and time bins. The relationship between the two matrices enables any observed sea condition to be immediately linked to the expected power output.

(a) Pelamis (power matrix)

Hs (m) \ Te (s)	5	5.5	6	6.5	7	7.5	8	8.5	9	9.5	10	10.5	11	11.5	12	12.5	13
0.5	0	0	0	0	0	0	0	0	0	0	0	0	0	0	0	0	0
1	0	22	29	34	37	38	38	37	35	32	29	26	23	21	0	0	0
1.5	32	50	65	76	83	86	86	83	78	72	65	59	53	47	42	37	33
2	57	88	115	136	148	153	152	147	138	127	116	104	93	83	74	66	59
2.5	89	138	180	212	231	238	238	230	216	199	181	163	146	130	116	103	92
3	129	198	260	305	332	340	332	315	292	266	240	219	210	188	167	149	132
3.5	0	270	354	415	438	440	424	404	377	362	326	292	260	230	215	202	180
4	0	0	462	502	540	546	530	499	475	429	384	366	339	301	267	237	213
4.5	0	0	544	635	642	648	628	590	562	528	473	432	382	356	338	300	266
5	0	0	0	739	726	731	707	687	670	607	557	521	472	417	369	348	328
5.5	0	0	0	750	750	750	750	750	737	667	658	586	530	496	446	395	355
6	0	0	0	0	750	750	750	750	750	750	711	633	619	558	512	470	415
6.5	0	0	0	0	750	750	750	750	750	750	750	743	658	621	579	512	481
7	0	0	0	0	0	750	750	750	750	750	750	750	750	676	613	584	525
7.5	0	0	0	0	0	0	750	750	750	750	750	750	750	750	686	622	593
8	0	0	0	0	0	0	0	750	750	750	750	750	750	750	750	690	625

(b) Bivariate distribution (site IE24)

Hs (m) \ Te (s)	5	5.5	6	6.5	7	7.5	8	8.5	9	9.5	10	10.5	11	11.5	12	12.5	13
0.5	0.389	0.789	0.758	1.06	0.885	0.489	0.281	0.185	0.177	0.0924	0.0077	0	0	0	0	0	0
1	0.504	1.3	2.1	2.15	2.32	1.7	1.68	0.727	0.643	0.485	0.139	0.119	0.0269	0.0231	0.00385	0	0
1.5	0.165	1.1	1.67	2.07	2.5	2.17	1.95	1.64	0.966	0.731	0.412	0.25	0.177	0.05	0.0962	0.0616	0
2	0	0.212	0.87	1.47	1.93	2.15	2.02	2.09	1.67	1.22	0.808	0.566	0.304	0.0462	0.0308	0.0346	0
2.5	0	0	0.239	0.65	1.24	1.64	1.45	1.87	1.92	1.46	1.31	0.974	0.573	0.327	0.127	0.0346	0
3	0	0	0.0269	0.196	0.596	1.2	1.44	1.62	1.63	1.14	0.804	0.812	0.454	0.416	0.385	0.1	0
3.5	0	0	0	0.0192	0.142	0.454	0.812	1.2	1.36	0.947	0.716	0.75	0.292	0.366	0.346	0.204	0
4	0	0	0	0	0.0269	0.0962	0.292	0.935	1.14	1.14	0.847	0.62	0.462	0.281	0.185	0.0385	0
4.5	0	0	0	0	0	0.0115	0.0693	0.296	0.581	0.543	0.546	0.377	0.308	0.316	0.319	0.0577	0
5	0	0	0	0	0	0.00385	0.00385	0.0924	0.231	0.381	0.354	0.404	0.223	0.285	0.223	0.158	0
5.5	0	0	0	0	0	0	0.00385	0.0269	0.0885	0.169	0.242	0.327	0.162	0.169	0.146	0.154	0
6	0	0	0	0	0	0	0	0	0.0269	0.123	0.223	0.123	0.223	0.0808	0.0962	0.108	0
6.5	0	0	0	0	0	0	0	0.0077	0	0.0231	0.112	0.0731	0.1	0.0731	0.0269	0.0423	0
7	0	0	0	0	0	0	0	0	0.00385	0.0154	0.0385	0.0616	0.0462	0.0462	0.0346	0.0423	0
7.5	0	0	0	0	0	0	0	0	0.00385	0.00385	0.05	0.0192	0.0192	0.0423	0.05	0.0346	0
8	0	0	0	0	0	0	0	0	0	0	0	0	0	0	0.00385	0	0

Figure 3. Specific matrixes related to: (**a**) Pelamis power matrix; and (**b**) bivariate distribution of the sea-state (in %) expected for the site IE24 (Ireland).

The primary goal of this work is to determine which wave parameters are more important for the performance of a specific WEC system. To do this, the EasyNN-plus program (version 10.0) was used to construct a correlation between various input data points (called predictors) and some outputs (called responses). The EasyNN program can handle up to three hidden layers, which are coupled together by a sigmoid activation function [15].

Figure 4 shows that the trained EasyNN model used eleven environmental and temporal inputs to generate three performance outputs: WEC power output, capacity factor, and capture width. These indicators were generated on a monthly basis, taking into account

the month, average, 10th percentile value, and maximum values (*Hs*, *Te*, and *Pw*), as well as the direction of the wave.

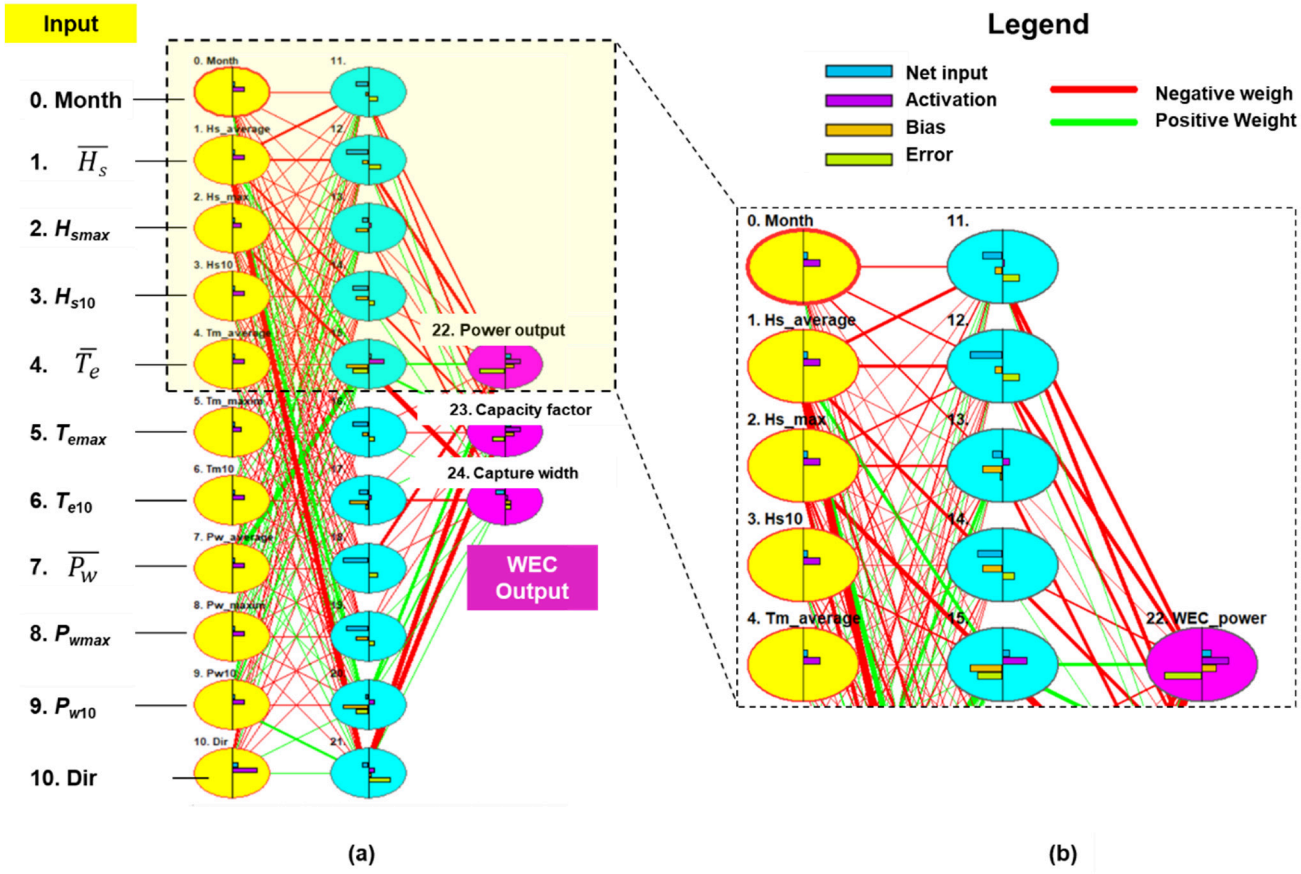

Figure 4. Overview of the EasyNN architecture, where (**a**) general overview; (**b**) detailed view indicating the connections between the nodes.

The present work used a cross-validation strategy to partition the given data into five subsets with a target error of 0.01%. In terms of hyperparameters, a momentum of 0.8 (decay) was used throughout the simulation; however, the learning rate can vary, as shown in Table 1. At this point, it should be noted that multiple combinations of the number of layers/nodes and hyperparameters are required to achieve valid results; therefore, only three years of ERA5 data were considered to reduce processing time effort. Table 1 shows that considering one or two hidden layers with various nodes allows for a broader number of layouts. The mean absolute error (MAE) will range from 0.014 to 0.030.

The target error is essential to achieve a valid result, although simulation accuracy is determined by the EasyNN software's importance and sensitivity features. More specifically, the two pieces of information must rank the input parameters in the same order; an ideal scenario would be a perfect match between all predictors. As seen in Table 2, it is not always possible to achieve a perfect match between importance and sensitivity. Given the large number of predictors, it was considered acceptable for the present work if at least five predictors overlapped; this approach has been used in prior investigations [16]. For this case study, the most important wave parameters are related to the average wave height and wave power, followed by the presence of the maximum wave heights.

Table 1. Overview of the EasyNN configuration and hyperparameters.

WEC	Hidden Layers		Learning Rate	MAE
	Layer 1 (Nodes)	Layer 2 (Nodes)		
		Site IE24 (Ireland)		
Wave Dragon	7	6	0.25 (decay)	0.020
Wave Bob	7	6	0.5 (decay)	0.026
Pelamis	11	0	0.5 (decay)	0.014
Ocentec	8	7	0.15 (no decay)	0.028
Seabased	8	0	0.27 (no decay)	0.015
		Site GEROA (France)		
Wave Dragon	19	3	0.25 (decay)	0.021
Wave Bob	17	2	0.2 (decay)	0.022
Pelamis	9	2	0.2 (decay)	0.027
Ocentec	12	3	0.2 (decay)	0.022
Seabased	7	6	0.2 (decay)	0.023
		Site Botafogo (Portugal)		
Wave Dragon	11	14	0.2 (decay)	0.019
Wave Bob	8	0	0.2 (decay)	0.021
Pelamis	15	7	0.6 (decay)	0.030
Ocentec	8	0	0.2 (decay)	0.028
Seabased	8	0	0.2 (decay)	0.017

Table 2. Performance indicator associated with the site IE24 and the Pelamis generator. The asterisk (*) indicate a correlation between importance and sensitivity.

WEC	Rank									
	1	2	3	4	5	6	7	8	9	10
					Site IE24 (Ireland)					
Importance	$\overline{H}_s$ *	$\overline{P}_w$ *	H_{smax} *	P_{w10} *	H_{s10} *	P_{wmax}	Month	T_{e10}	*Dir*	$\overline{T}_e$
Value	12.49	9.48	8.74	6.52	5.46	4.84	4.53	4.37	3.37	3.17
Sensitivity	$\overline{H}_s$ *	$\overline{P}_w$ *	H_{smax} *	P_{w10} *	H_{s10} *	T_{emax}	$\overline{T}_e$	P_{wmax}	Month	T_{e10}
Value	0.19	0.10	0.041	0.040	0.040	0.03	0.01	0.01	0	0

3. Results

A preliminary assessment of the wave conditions, considering the *Hs* and *Te* parameters, is given in Figure 5. It is evident from the monthly distribution of the average *Hs* (Figure 5a) that the site IE24 (Ireland) is characterised by more significant resources, which can reach 4.19 m in December. Botafogo (Portugal) can be ranked second, while much lower values are anticipated close to GEROA (France), which makes sense given that this location is not directly exposed to ocean waves.

The locations under consideration exhibit a comparatively similar monthly distribution in terms of the wave period (Figure 5b), with the exception that the site Botafogo is generally characterised by a substantially higher wave period. The histograms show that the GEROA site (interval 1–2 m) has a peak, and the *Hs* values (Figure 5c) are grouped in the interval 1–4 m. A normal distribution with values centred around the 8–10 s interval is observed when we shift to the wave period (Figure 5d).

Table 3 provides a more complete study of the wave conditions, including wave power. These data are structured for the full-time distribution (denoted by TT) as well as the key seasons, which are: (a) MAM (March–April–May); (b) JJA (June–July–August); (c) SON (September–October–November); and (d) DJF (December–January–February). In general, the winter season is more energetic, with a maximum of 11.3 m recorded at

the IE24 location. The *Hs* standard deviation (or *Std*) is defined as a minimum value of 0.43 m at the GEROA and Botafogo sites (season JJA). The standard deviation for the *Te* parameter is between 1.23 and 2.29 s, depending on the season and site. The site IE24 is distinguished by significantly higher wave power, which in the event of average values can reach a maximum of 207 kW/m (DJF season), compared to 103 and 130 kW/m at the other two sites.

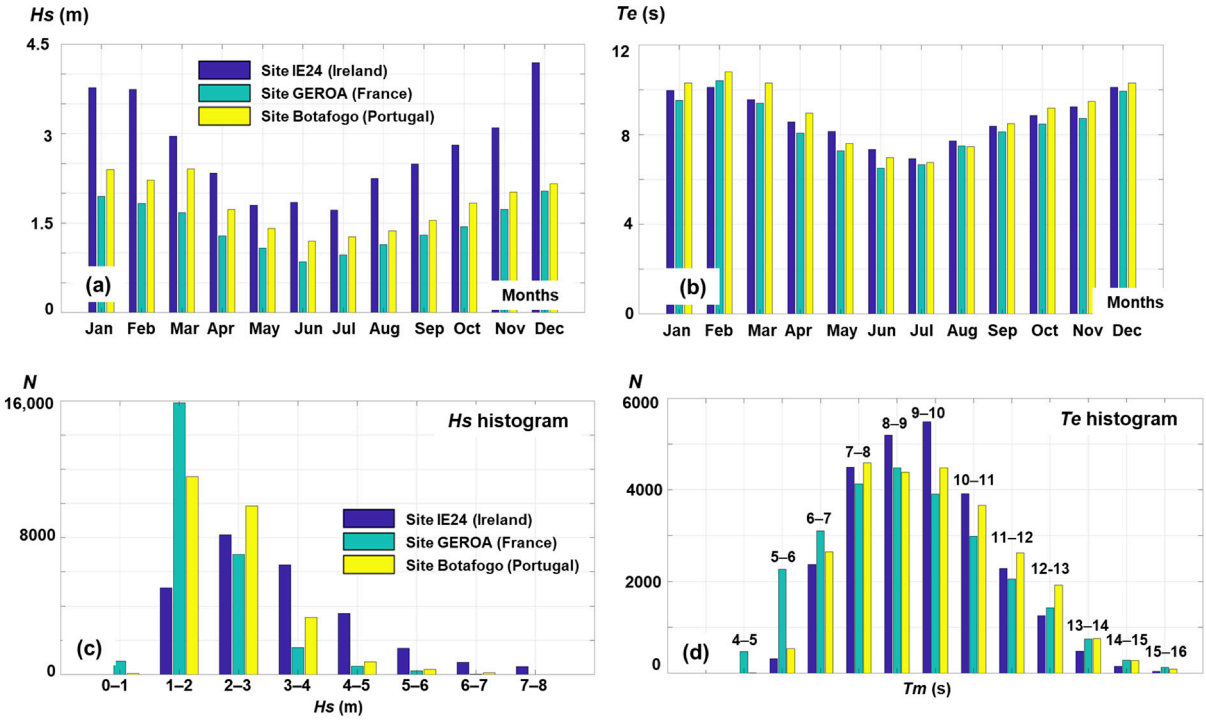

Figure 5. Wave statistics based on 3 years of ERA5 data, where (**a**) monthly average of *Hs*; (**b**) monthly average of *Te*; (**c**) *Hs* histogram; and (**d**) *Te* histogram.

Table 3. Wave statistics based on different time intervals.

Point	Interval	*Hs* (m)			*Te* (s)			*Pw* (kW/m)		
		Mean	*Std*	Extreme	Mean	*Std*	Extreme	Mean	*Std*	Extreme
IE24	TT	2.73	1.41	11.3	8.72	1.78	15.2	118	107	895
	MAM	2.36	1.12	7.23	8.76	1.62	14.8	98.5	76	557
	JJA	1.94	0.93	6.83	7.33	1.23	13.9	57.1	53.3	627
	SON	2.8	1.22	9.77	8.82	1.55	14	116	86	811
	DJF	3.89	1.55	11.3	10.10	1.58	15.2	207	137	895
GEROA	TT	1.43	0.80	6.2	8.35	2.26	16.4	60	60.8	480
	MAM	1.35	0.65	4.45	8.24	1.94	13.7	51.5	44.3	322
	JJA	0.99	0.43	3.61	6.89	1.74	16.1	27.3	27.6	289
	SON	1.49	0.80	5.81	8.44	1.98	13.9	60.4	55.6	480
	DJF	1.94	0.93	6.2	9.94	2.29	16.4	103	78.8	480
Botafogo	TT	1.79	0.87	6.7	8.85	2.03	15.3	80.2	71.9	646
	MAM	1.85	0.81	6.33	8.95	1.77	15.1	80.4	60.5	383
	JJA	1.28	0.43	3.43	7.06	1.26	15.1	33.9	26.9	319
	SON	1.8	0.88	6.7	9.04	1.61	14.3	79.7	66.8	646
	DJF	2.27	0.95	6.46	10.4	1.84	15.3	130	86.6	514

The distribution of the wave roses, taking into account all available values, is shown in Figure 6. In contrast to GEROA and Botafogo, where northwest waves predominate, site IE24 is characterised by waves originating from the western sector.

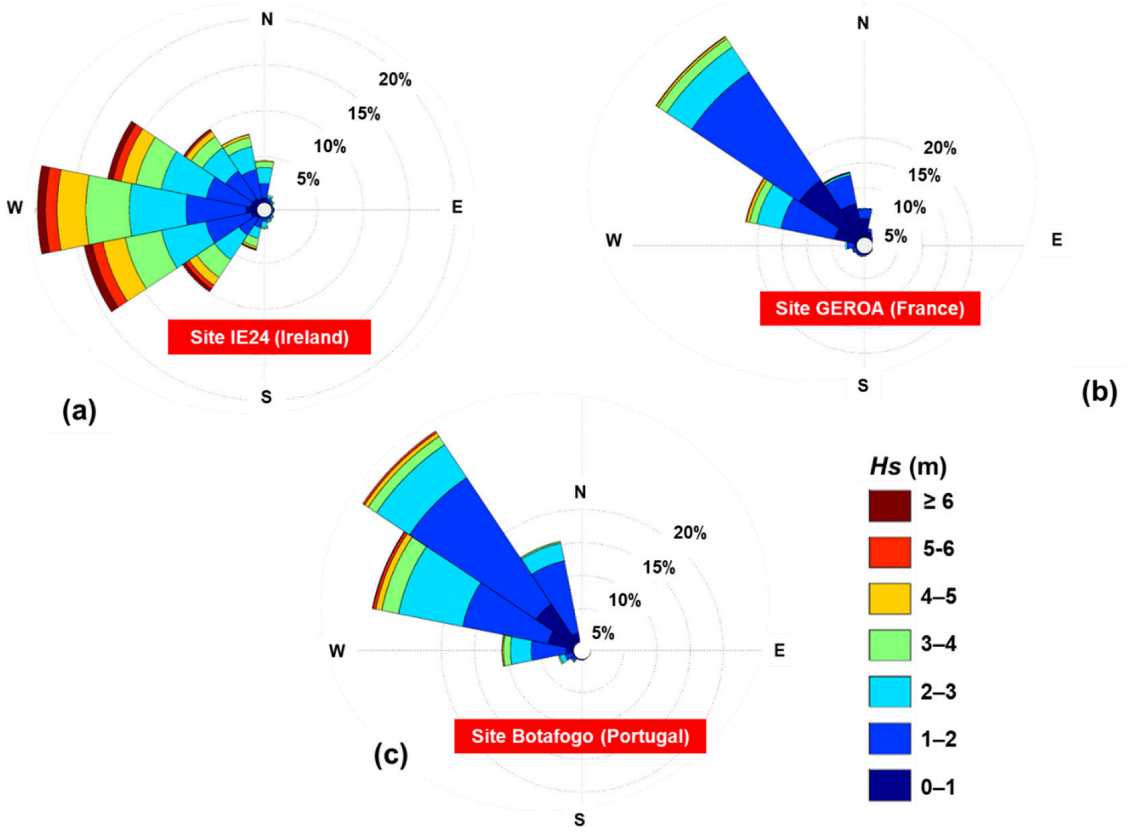

Figure 6. Wave roses (total time) indicated in terms of the *Hs* classes, where (**a**) site IE24; (**b**) site GEROA; and (**c**) site Botafogo.

Table 4 displays the outcomes of neural network simulations (EasyNN) for the IE24 site in Ireland. For instance, the Wave Dragon system showed an overlap of 10 predictors, which is higher compared to only five predictors found for both Pelamis and Oceantec systems.

Table 4. Site IE24 (Ireland)—WEC similarity between importance and sensitivity indexes.

WEC	Rank									
	1	**2**	**3**	**4**	**5**	**6**	**7**	**8**	**9**	**10**
Wave Dragon	$\overline{Hs}$	$\overline{P}_w$	Hs_{10}	P_{w10}	$\overline{T}_e$	P_{wmax}	Te_{10}	Te_{max}	Hs_{max}	Month
Wave Bob	$\overline{H}_s$	$\overline{P}_w$	Hs_{max}	*Dir*	$\overline{T}_e$	Pw_{10}	-	-	-	-
Pelamis	$\overline{Hs}$	$\overline{P}_w$	Hs_{max}	Pw_{10}	Hs_{10}	-	-	-	-	-
Ocentec	Pw_{10}	Hs_{10}	Month	$\overline{Hs}$	Hs_{max}	-	-	-	-	-
Seabased	$\overline{Hs}$	$\overline{P}_w$	Hs_{max}	Hs_{10}	Pw_{10}	Month	-	-	-	-

The wave direction generally does not play a significant role, except in the case of the Wave Bob system. In contrast, the distribution of months appears to have a stronger impact. In general, the average wave height, average wave power, and maximum wave height are listed first. However, in the case of the Oceantec, the 10th percentile of wave power and height is more essential, followed by the monthly evolution of the sea state. In the instance of the Wave Dragon, we can plainly see that the less important characteristics are associated with the maximum wave duration and wave heights, while the monthly influence appears to be minimal.

https://doi.org/10.3390/engproc2026152019

Table 5 shows a similar analysis for the GEROA site, with only the Seabased system exhibiting a high similarity hierarchy. In comparison to the previous page, the average wave power for the Wave Dragon and Pelamis is listed first. Extreme values (Pw_{max} and Hs_{max}) will have a substantial impact on the Oceantec system's electricity generation. The 10th percentile values have less influence on this site, with some contributions predicted from Pelamis (Pw_{10}) and Seabased (Te_{10}). In the case of a sea-based generator (point absorber), the wave period is less relevant for energy production.

Table 5. Site GEROA (France)—WEC similarity between the importance and sensitivity indexes.

WEC	Rank									
	1	**2**	**3**	**4**	**5**	**6**	**7**	**8**	**9**	**10**
Wave Dragon	$\overline{Pw}$	$\overline{H}_s$	Pw_{max}	Hs_{10}	Pw_{10}	-	-	-	-	-
Wave Bob	$\overline{Hs}$	$\overline{Pw}$	Te_{max}	Hs_{max}	Pw_{max}	-	-	-	-	-
Pelamis	$\overline{P}_w$	$\overline{Hs}$	Pw_{max}	Pw_{10}	Hs_{max}	Te_{10}	-	-	-	-
Ocentec	$\overline{Hs}$	Pw_{max}	$\overline{Pw}$	Hs_{max}	$\overline{T}_e$	-	-	-	-	-
Seabased	$\overline{Hs}$	$\overline{P}_w$	Pw_{max}	Te_{10}	Hs_{max}	Hs_{10}	Pw_{10}	*Month*	$\overline{T}_e$	Te_{max}

Table 6 shows a similarity analysis for the site Botafogo. Regardless of the WEC used, the *Hs* parameter (average, maximum, or tenth) was obtained first, and we can add the average wave power from there. In the case of the wave period, the average and tenth percentile values are more essential. Another key element is that the wave direction and months are not provided as relevant for the WEC systems under consideration.

Table 6. Site Botafogo (Portugal)—WEC similarity between the importance and sensitivity indexes.

WEC	Rank					
	1	**2**	**3**	**4**	**5**	**6**
Wave Dragon	$\overline{H}_s$	$\overline{P}_w$	Hs_{max}	Hs_{10}	Te_{10}	-
Wave Bob	$\overline{H}_s$	Hs_{max}	Hs_{10}	$\overline{P}_w$	Pw_{10}	$\overline{T}_e$
Pelamis	$\overline{Hs}$	$\overline{P}_w$	Hs_{max}	Te_{max}	Pw_{max}	-
Ocentec	Hs_{max}	$\overline{Hs}$	$\overline{Pw}$	Pw_{max}	Te_{max}	-
Seabased	$\overline{Hs}$	$\overline{P}_w$	Hs_{max}	Hs_{10}	Te_{10}	Pw_{max}

4. Conclusions

The EasyNN neural network can be applied to a broader range of applications, including renewable systems [17–19]. To obtain a valid result, two conditions must be met: (a) The target error is less than 0.01; and (b) the importance and sensitivity indices are similar. To accomplish this, we must test alternative network topologies while taking into account the model's specific parameters (for example, learning rate).

Given the number of offshore sites (and WECs) involved, it was decided to use only three years of ERA5 hourly data (2023–2025) to decrease processing time. An acceptable result was reached when at least five importance/sensitivity parameters showed the same hierarchy. It is possible to get a 100% association between the predictors, but this requires the use of an embedded evolutionary generator [20,21].

The chosen sites are located in European coastal areas distinguished by certain characteristics. In terms of wave energy resources, the IE24 site is located in one of the most promising coastal areas for exploiting these natural resources, followed by other sites such as Portugal [22]. The Bay of Biscay (GEROA site) is also seen as a viable place for wave energy, given the operation of the Mutriku wave energy plant (296 kW) [23]. Although just three years of ERA5 data were used, the statistical results confirm the overall distribution of wave energy, which decreases steadily from the north (Ireland) to the Iberian Peninsula.

To construct a valid long-term trend in ocean wave data, at least 30 years of data are often necessary [24,25]. The performance of WEC systems can be identified by using a considerably smaller dataset. For example, in the work of Wells et al. [26], which focused on the Wadden Sea (Dutch coast), only 10 years of data were utilised to determine the performance of wave farms. However, for deep learning research, a significantly smaller dataset is typically required. This is the case in the work done by Kim et al. [27], who used only four years of ERA5 data to predict the radiative flux forecast in the Arctic. Zanchi et al. [28] proposed a similar approach, using only two years of ERA5 data to forecast microclimate conditions. The performance of WEC systems can be evaluated from a variety of perspectives (e.g., design, optimisation), as demonstrated by Valério et al. [29], who used only one year of data to run multiple neural network models for control techniques.

As previously stated, because the EasyNN results are not straightforward and involve numerous "test and run" approaches, only three years of hourly ERA5 data were analysed in the current work. This can be viewed as a limitation of the current study, despite the fact that different sites and WEC generators were evaluated.

The primary goal of this study was to determine which wave characteristic is more essential for the performance of a specific WEC, while taking into account diverse European coastal areas related to the ocean environment. In general, the performance of WECs is related to the average values of wave heights and wave power, with less effect from wave period. This appears to be counterintuitive given that each WEC's power matrix is based on the combination of wave height and wave period. Among the other essential wave parameters, we may find highest values of *Hs* (sites IE24 and Botafogo) and *Pw* (site GEROA). Regarding the functioning principle, the Wave Dragon (terminator), the market's largest WEC, is less affected by the maximum *Hs* and *Te*, a certain month, or wave orientation. For an attenuator system (Pelamis), the 10 percentile values of *Hs* and *Pw* appear to be important for the sites IE24 and GEROA, but extreme values are more relevant for Botafogo. In terms of temporal relevance, the monthly influence is most obvious on the site IE24 (Ireland), while the importance of wave direction should also be mentioned (Wave Bob system).

Finally, we may highlight that the current work is continuous, and future improvements can be made. To anticipate the long-term performance of a WEC system, at least ten years of data must be analysed for future simulation. Taking into account some other neural networks will be another important aspect.

Author Contributions: R.-A.D. and O.F. performed the literature review, processed the data, and wrote the manuscript. E.R. designed and supervised the present work. All authors have read and agreed to the published version of the manuscript.

Funding: This research received no external funding.

Institutional Review Board Statement: Not applicable.

Informed Consent Statement: Not applicable.

Data Availability Statement: Dataset available on request from the authors.

Acknowledgments: The ERA5 wind dataset was downloaded from the Copernicus Climate Change Service (C3S) Climate Data Store.

Conflicts of Interest: The authors declare no conflicts of interest.

References

1. Amir, M.A.U.; Sharip, R.M.; Muzanni, M.A.; Anuar, H.A. *Wave Energy Convertors (WEC): A Review of the Technology and Power Generation*; AIP Publishing: Songkhla, Thailand, 2016; p. 030100.

2. Drew, B.; Plummer, A.R.; Sahinkaya, M.N. A Review of Wave Energy Converter Technology. *Proc. Inst. Mech. Eng. Part J. Power Energy* **2009**, *223*, 887–902. [CrossRef]
3. Bouhrim, H.; El Marjani, A.; Nechad, R.; Hajjout, I. Ocean Wave Energy Conversion: A Review. *J. Mar. Sci. Eng.* **2024**, *12*, 1922. [CrossRef]
4. Azam, A.; Ahmed, A.; Yi, M.; Zhang, Z.; Zhang, Z.; Aslam, T.; Mugheri, S.A.; Abdelrahman, M.; Ali, A.; Qi, L. Wave Energy Evolution: Knowledge Structure, Advancements, Challenges and Future Opportunities. *Renew. Sustain. Energy Rev.* **2024**, *205*, 114880. [CrossRef]
5. Ozkop, E.; Altas, I.H. Control, Power and Electrical Components in Wave Energy Conversion Systems: A Review of the Technologies. *Renew. Sustain. Energy Rev.* **2017**, *67*, 106–115. [CrossRef]
6. Atlantic Marine Energy Test Site (AMETS). Available online: https://openei.org/wiki/PRIMRE/Databases/Projects_Database/Test_Sites/Atlantic_Marine_Energy_Test_Site_(AMETS) (accessed on 24 September 2026).
7. GEROA Floating Offshore Wind Farm. Available online: https://www.gem.wiki/GEROA_Floating_Offshore_wind_farm (accessed on 24 September 2026).
8. Botafogo Floating Wind | IberBlue Wind. Available online: https://www.iberbluewind.com (accessed on 24 September 2026).
9. ERA5 Hourly Data on Single Levels from 1940 to Present. Available online: https://cds.climate.copernicus.eu/datasets/reanalysis-era5-single-levels?tab=overview (accessed on 24 September 2026).
10. Rusu, E.; Onea, F. Estimation of the Wave Energy Conversion Efficiency in the Atlantic Ocean Close to the European Islands. *Renew. Energy* **2016**, *85*, 687–703. [CrossRef]
11. Provenza, B.; Guercio, A.; Curto, D.; Franzitta, V. Wave Energy Converters: A State-of-the-Art Review of Wave-Activated Body Technologies. *J. Mar. Sci. Eng.* **2026**, *14*, 1777. [CrossRef]
12. Majidi, A.G.; Ramos, V.; Rosa-Santos, P.; das Neves, L.; Taveira-Pinto, F. Power Production Assessment of Wave Energy Converters in Mainland Portugal. *Renew. Energy* **2025**, *243*, 122540. [CrossRef]
13. Onea, F.; Rusu, E.; Rusu, L. Assessment of Wave Energy Converter Performance with Satellite Data. *J. Mar. Sci. Eng.* **2026**, *14*, 1208. [CrossRef]
14. Rusu, L.; Onea, F. The Performance of Some State-of-the-Art Wave Energy Converters in Locations with the Worldwide Highest Wave Power. *Renew. Sustain. Energy Rev.* **2017**, *75*, 1348–1362. [CrossRef]
15. Mereuta, E.; Novetschi, M.-I.; Ganea, D.; Amortila, V.T.; Nazer, T. Validation of the Mathematical Model of Upper Body Biomechanics Using Neural Networks. *Balneo PRM Res. J.* **2024**, *15*, 690. [CrossRef]
16. Bălășoiu, G.; Munteniță, C.; Amortila, V.T.; Titire, L. Optimisation of Clutch Disc Friction Material Using a Multi-Layer Perceptron Artificial Neural Network. *Polymers* **2024**, *16*, 3588. [CrossRef] [PubMed]
17. Ciortan, S.; Rusu, E. Prediction of the Wave Power in the Black Sea Based on Wind Speed Using Artificial Neural Networks. *E3S Web Conf.* **2018**, *51*, 01006. [CrossRef]
18. Lobato-Nostroza, O.; Chávez-Campos, G.M.; Morales-Cervantes, A.; Chiaradia-Masselli, Y.M.; Lara-Hernández, R.; Téllez-Anguiano, A.D.C.; Fraga-Aguilar, M. Predictive Modeling of Photovoltaic Panel Power Production through On-Site Environmental and Electrical Measurements Using Artificial Neural Networks. *Metrology* **2023**, *3*, 347–364. [CrossRef]
19. Fonseca, R.W.D.; Pereira, F.O.R. Metamodeling of the Energy Consumption of Buildings with Daylight Harvesting—Application of Artificial Neural Networks Sensitive to Orientation. *J. Daylighting* **2021**, *8*, 255–269. [CrossRef]
20. Stăvărache, G.; Ciortan, S.; Rusu, E. Optimization of Artificial Neural Networks Based Models for Wave Height Prediction. *E3S Web Conf.* **2020**, *173*, 03007. [CrossRef]
21. Ezpeleta, H.; Ulazia, A.; Aristondo, O.; Ibarra-Berastegi, G. Future Wave Energy Evolution in the Bay of Biscay for Different Converters. *Energy* **2025**, *331*, 136713. [CrossRef]
22. O'Connell, R.; Murphy, J. Offshore Wind and Wave Energy on the European Atlantic Shelf: A Multi-Decadal High-Resolution Metocean Analysis. *Appl. Ocean Res.* **2026**, *173*, 105180. [CrossRef]
23. Ibarra-Berastegi, G.; Ulazia, A.; Sáenz, J.; Serras, P.; González Rojí, S.J.; Esnaola, G.; Iglesias, G. The Power Flow and the Wave Energy Flux at an Operational Wave Farm: Findings from Mutriku, Bay of Biscay. *Ocean Eng.* **2021**, *227*, 108654. [CrossRef]
24. Sun, P.; Xu, B.; Wang, J. Long-Term Trend Analysis and Wave Energy Assessment Based on ERA5 Wave Reanalysis along the Chinese Coastline. *Appl. Energy* **2022**, *324*, 119709. [CrossRef]
25. Kardakaris, K.; Dimitriadis, P.; Iliopoulou, T.; Koutsoyiannis, D. Stochastic Simulation of Wind Wave Parameters for Energy Production. *Ocean Eng.* **2023**, *274*, 114029. [CrossRef]
26. Wells, S.; Alday, M.; Ilzarbe, J.M.B.; Lavidas, G. Assessing the Impact of WEC Arrays on the Nearshore Wave Climate and Power Production on the Dutch Coast. *Energy* **2025**, *331*, 136698. [CrossRef]
27. Kim, D.-H.; Kim, H.M. Deep Learning for Downward Longwave Radiative Flux Forecasts in the Arctic. *Expert Syst. Appl.* **2022**, *210*, 118547. [CrossRef]

28. Zanchi, M.; Zapperi, S.; La Porta, C.A.M. Harnessing Deep Learning to Forecast Local Microclimate Using Global Climate Data. *Sci. Rep.* **2023**, *13*, 21062. [CrossRef] [PubMed]
29. Valério, D.; Mendes, M.J.G.C.; Beirão, P.; Sá Da Costa, J. Identification and Control of the AWS Using Neural Network Models. *Appl. Ocean Res.* **2008**, *30*, 178–188. [CrossRef]

Disclaimer/Publisher's Note: The statements, opinions and data contained in all publications are solely those of the individual author(s) and contributor(s) and not of MDPI and/or the editor(s). MDPI and/or the editor(s) disclaim responsibility for any injury to people or property resulting from any ideas, methods, instructions or products referred to in the content.